

High performance multimode interference couplers for coherent communications in silicon

R. Halir*^a, G. Roelkens^b, A. Ortega-Moñux^a, J. G. Wangüemert-Pérez^a, I. Molina-Fernández^a
^aETSI Telecomunicación, Universidad de Málaga, 29010 Málaga, Spain;
^bINTEC, Ghent University-Interuniversity Microelectronics Center, 9000 Gent, Belgium

ABSTRACT

We review the need for coherent optical communication systems and briefly describe the receiver frontend they require. The key element of the receiver is an optical 90° hybrid, which combines the received signal with the local oscillator laser with the adequate amplitude and phase relations. Silicon technology offers several advantages for the realization of such devices: compactness and CMOS compatibility, among others. However, the realization of high-performance hybrids is hampered by the high index contrast of this technology. We show that using multimode interference couplers with fully etched access waveguides and a shallowly etched multimode region, ultra-compact, high performance 90° hybrids can be realized. We experimentally demonstrate a device with a phase error below 5° and a common mode rejection ratio better than -20dB in a ~50nm bandwidth.

Keywords: coherent communications, silicon photonics, 90° hybrid, multimode interference coupler

1. INTRODUCTION

Current fiber optic transmission systems were deployed for data transmission at 10Gbit/s per carrier using on-off keying, with a channel spacing of 50GHz. The growing demand for high speed data transmission calls for a tenfold increase in per carrier transmission rates, to 100Gbit/s or even 400Gbit/s. Use of conventional on-off keying would require an equally ten-fold increase in transmission bandwidth to achieve such data rates, yielding signals that cannot be transmitted over the existing infrastructure. However, by moving from on-off keying to more advanced coherent modulations, 100Gbit/s transmission over the currently deployed 50GHz infrastructure is feasible, since only the transmitter and receiver end need be upgraded.¹ However, both the coherent receiver and transmitter exhibit a considerable complexity, especially when compared to the devices used for on-off keying. Integrated optical solutions are thus ideally suited for the implementation of coherent transmitters and receivers, and furthermore offer potentially high volume, low cost fabrication. In this communication we focus on the implementation of coherent optical receivers in the Silicon-on-Insulator platform, which enables ultra-compact designs and CMOS compatible fabrication. Specifically, we discuss the design and experimental characterization of high performance 2x4 multimode interference couplers that act as 90° hybrids, and constitute the core of coherent optical receivers. We experimentally demonstrate a phase error below 5° and a common mode rejection ratio below -20dB in a ~50nm bandwidth, with a device that occupies less than 135μm x 8μm.

This paper is organized as follows. In section 2 we succinctly describe the concept of coherent optical communications and in section 3 we briefly examine the main elements of a coherent optical receiver frontend, paying special attention to 90° hybrids. We then focus on the implementation of 90° hybrids with multimode interference couplers (section 4), and discuss the details of their design in ultra-compact silicon-wire waveguides in section 5. We describe our design approach in section 6, where we also present the experimental results. Finally, conclusions are drawn in section 7.

2. COHERENT OPTICAL COMMUNICATIONS

In order to transmit 100Gbit/s over the 50GHz bandwidth available in the current infrastructure, both advanced modulation formats, and polarization multiplexing are used.

*robert.halir@ic.uma.es; phone +34 952 13 2853; www.ic.uma.es

Advanced modulation formats, such as quadrature phase shift keying (QPSK), are used to convey two (or more) bits in each transmitted symbol. This is achieved by splitting the transmitting laser in two paths, with a 90° phase shift between them, yielding a cosine and a sine wave. These waves are orthogonal and are commonly referred to as the I (in-phase) and Q (quadrature) channels. Each channel is modulated separately with information bits, and both modulated waves are then combined again. As shown in Fig. 1(a), for a QPSK modulation this enables simultaneous transmission of two bits (one in the I channel and one in the Q channel), thereby reducing the required bandwidth by a factor of two. In order to recover the data, a coherent receiver is required. Such a receiver recovers both amplitude and phase of the transmitted signal, by having it interfere with a local oscillator laser.

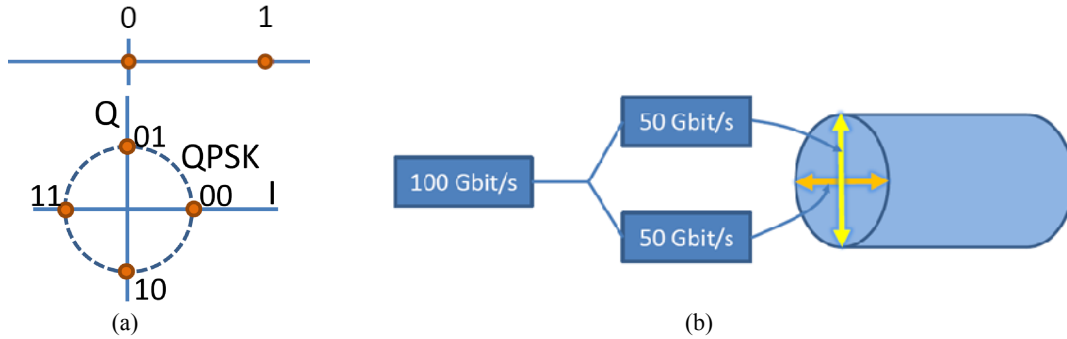


Figure 1. (a) On-off keying constellation compared to a QPSK constellation. (b) Polarization multiplexing concept.

Polarization multiplexing consists in transmitting one half of the data stream in the vertical polarization state of the fiber, and the other half in the horizontal polarization state [see Fig. 1(b)]. At the receiver end, a polarization splitter is used to separate the horizontal and vertical polarization states. Since optical fibers randomly rotate the polarization state of light, the horizontal and vertical polarization states at the receiver end do not correspond with the states at the transmitter, and the transmitted data cannot be directly recovered. However, since the coherent receiver recovers both the amplitude and phase information of the transmitted field, digital signal processing algorithms can be used to restore the proper polarization axes.¹

3. RECEIVER FRONTEND

The mission of the coherent receiver frontend is to mix the received signal with a local oscillator laser with specific phase relations, and produce electrical output signals which are, ideally, the data streams in the I and Q channels for both polarizations. As shown schematically in Fig. 2(a), the receiver frontend consists of a polarization management part, possibly comprising polarization splitters (PBS) and polarization converters (PC), optical 90° hybrids that combine the received signal and the local oscillator laser with the required amplitude and phase relations, and differential (bipolar) photo diodes (BPD), that convert the optical signal to the electrical domain. Here we will focus on the realization of the 90° hybrids.

The 90° hybrid has to combine the received signal, S , and the local oscillator laser, LO , as defined in Fig. 2(b).² At each output, numbered 3, 4, 5 and 6 in Fig. 2(b), the two input signals are combined with the same amplitude but with phase shifts that are offset by exactly 90°. Differential detection of the output pairs (3,6) and (4,5) gives the I and Q channel, from which, upon digital post-processing, the transmitted data can be extracted. The specifications of 90° hybrids for coherent optical reception are given in terms of common mode rejection ratio and phase error.³ Denoting by p_i the power at each output when light is launched either into input 1 or 2, the CMRR for the I and Q channel is defined as:

$$\begin{aligned}
 \text{CMRR}_I [\text{dBe}] &= 20 \log_{10} \frac{p_3 - p_6}{p_3 + p_6} \\
 \text{CMRR}_Q [\text{dBe}] &= 20 \log_{10} \frac{p_4 - p_5}{p_4 + p_5}
 \end{aligned} \tag{1}$$

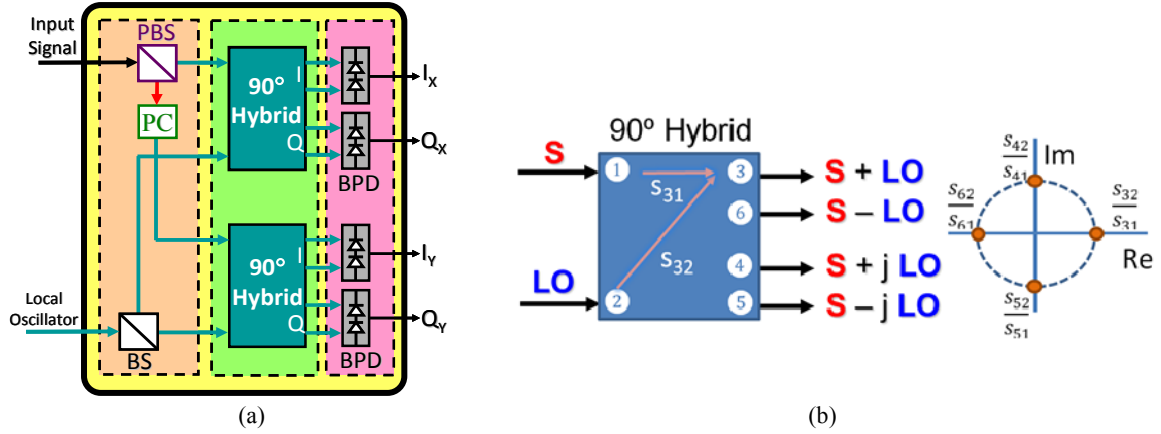


Figure 2. (a) Schematic illustration of the receiver frontend. (b) Operation of the 90° Hybrid.

The factor 20 here is due to the definition in electrical decibels. The phase error (PE) is defined in terms of ϕ , which is the relative phase with which waves from inputs 1 and 2 combine at outputs $i=3,4,5,6$:

$$\begin{aligned}
 PE_{63} &= \left| \phi_6 - \phi_3 - 180^\circ \right| \\
 PE_{54} &= \left| \phi_5 - \phi_4 - 180^\circ \right|. \\
 PE_{65} &= \left| \phi_6 - \phi_5 - 90^\circ \right|
 \end{aligned} \tag{2}$$

Specifications require the CMRR to be below -20dBe and all phase errors to be smaller than 5°.

4. MULTIMODE INTERFERENCE COUPLERS BASED 90° HYBRIDS

Several configurations of multimode interference couplers (MMIs) can be used to implement 90° hybrids^{2,4}, and while other devices, such as star couplers⁵ can also be employed, MMIs are generally preferred because of their relatively broad bandwidth, and more relaxed fabrication tolerances.⁶ Specifically, a 4x4 MMI, where, as shown in Fig. 3, two input ports (1 and 2) and four output ports (3,4,5,6) are used, constitute a fully passive realization of a 90° hybrid. This is the structure we will focus on in the following, even though the concepts we discuss are valid for MMIs in general.

The operation of MMI couplers is based on the self-imaging which can be described as follows. When light is launched into one of the input waveguides (1 or 2 in Fig. 3), it excites multiple higher order modes in the central multimode region. These higher order modes have different propagation constants, β_m , and interfere as they propagate along the multimode region. At certain distances, the interference forms multiple replicas or images of the input excitation. By properly placing the output waveguides the images couple into the waveguides, yielding the desired behavior. However, for high quality imaging three conditions must be fulfilled:⁶

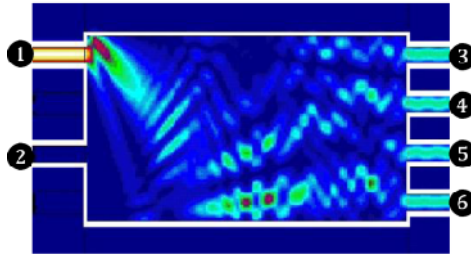


Figure 3. Light propagating through a 4x4 MMI coupler, where only the ports numbered from 1 to 6 are used.

1. Self-Imaging theory assumes a two-dimensional device model that only takes into account the lateral and propagation directions. This implies that all effects that occur in the vertical direction, will, in principle, have a negative impact on image quality, and, consequently, on device performance.
2. Only guided modes should be excited in the multimode region, since all the power that couples into radiation modes will necessarily be lost.
3. The modes propagating in the multimode region should be paraxial; specifically their propagation constants, β_m , should be related as:

$$\beta_m = \beta_1 - (m^2 - 1) \frac{\pi}{3L}, \quad (3)$$

where $L = \pi/(\beta_1 - \beta_2)$. Any deviation from this relation will result in modal phase errors at the end of the multimode region, so that the interference of the modes will not take place with the proper (modal) phases, resulting in poor image quality.

5. HIGH QUALITY IMAGING IN SI-WIRE WAVEGUIDES

Silicon wire technology is a highly attractive platform for the implementation of optical hybrids. Because of its small waveguide core and high index contrast (see Fig. 4), it allows for ultra-small devices and tight bending radii ($R \sim 5 \mu\text{m}$), enabling complex interconnections. Furthermore, a complete receiver frontend, as described in section 3, can be implemented in this technology, using polarization splitting fiber-to-chip grating couplers^{7,8} and germanium based photodetectors.⁹

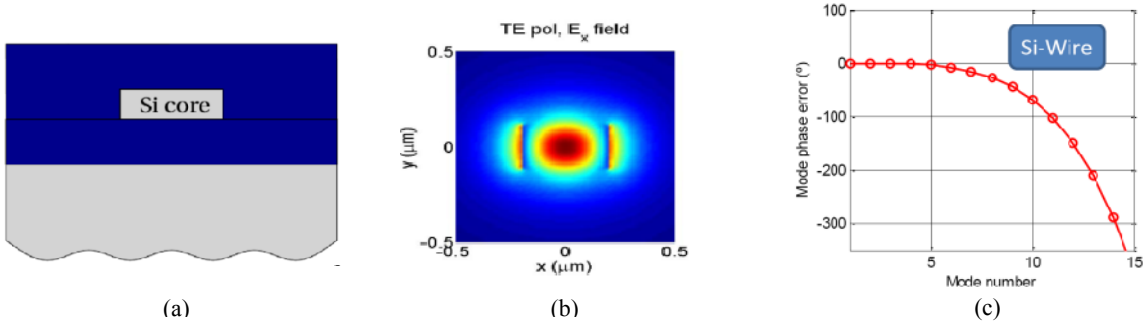


Figure 4. (a) Schematic cross-section of a silicon-wire waveguide. The silicon waveguide core is 450nm wide and 220nm thick, with an index contrast of $\Delta n \approx 2$ between the core and cladding. (b) TE mode field of a Si-wire waveguide. (c) Modal phase error in a silicon wire waveguide.

We will now analyze if the three conditions required for high quality imaging described in the previous section are fulfilled in silicon-wire waveguides.

1. Fig. 4(b) shows the TE mode field of a silicon wire waveguide. Clearly the field is symmetric in the vertical (y) direction. Consequently no information is lost when considering only the two dimensional model.
2. The excitation of radiation modes mainly depends on the width of the input waveguides.¹⁰ The narrower the waveguide, the wider is the plane wave spectrum of its fundamental mode. Energy travelling in angles of the plane wave spectrum that are larger than the critical angle of the lateral interface of the multimode region will be lost in form of radiation.
3. The modal phase errors in the multimode region depends directly on the index contrast.¹¹ As shown in Fig. 4(c), the high index contrast of Si-wire waveguides introduces critically high modal phase errors, especially for the higher order modes.

The use of significantly widened access waveguides has been shown to yield improved MMI performance.^{10,12,13} This can be understood as follows: wide waveguides avoid not only the excitation of radiation modes, but also of the highest order modes of the multimode section, which exhibit the strongest phase errors. However, this approach sacrifices the

compactness typical for Si-wire circuits. In the following section we propose a novel structure that overcomes these limitations.

6. COMPACT, HIGH PERFORMANCE 90° HYBRID IN SI-WIRE WAVEGUIDES

The design approach we propose is illustrated in Fig. 5(a). We employ a shallowly etched multimode region, thereby reducing the lateral index contrast, which allows us to control the modal phase error in the MMI. Fig. 5(b) shows the modal phase error as a function of the height of the lateral, shallowly etched slab. A slab height of $h=150\text{nm}$ results in the lowest phase error for the 220nm thick silicon layer we used. Furthermore, fully etched input and output waveguides are used, which drastically reduces coupling between them, allowing for a denser spacing, and, hence, for an overall smaller device. Direct interfacing of the shallowly etched multimode region with the fully etched access waveguides is possible with minimal losses, because, as shown in Fig. 5(c), the mode fields of both waveguides exhibit the same symmetry.¹⁴

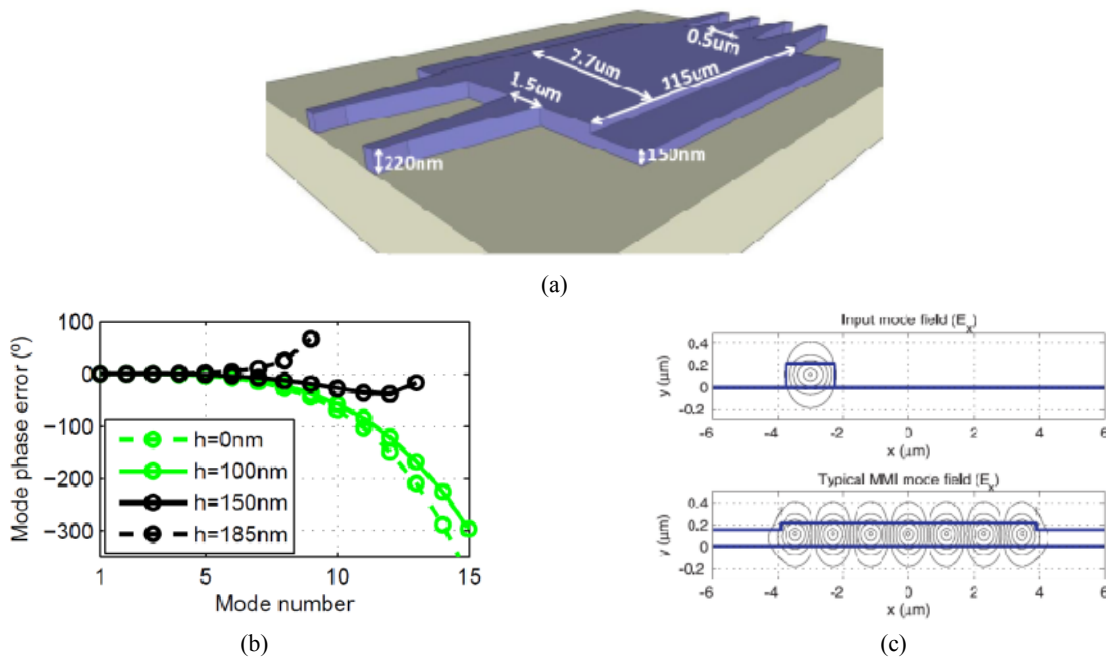


Figure 5. (a) Geometry of our MMI design, with a shallowly etched multimode region and fully etched access waveguides. (b) Modal phase error as a function of the height of the lateral slab of the multimode region. (c) Comparison of the mode field of the input waveguide and one of the higher order modes of the multimode region.

The device was fabricated within the ePIXfab network¹⁵, on an SOI wafer with a silicon thickness of 220 nm. Structures were defined with 193nm deep UV lithography and a two etch depth process. A 70 nm etch was used for the multimode region and the fiber-to-chip grating couplers, whereas the photonic wires were fully etched. Fiber-to-chip coupling was performed with grating couplers.¹⁶ To facilitate the measurement of the hybrids phase response, it was embedded in the on-chip interferometer shown in Fig. 6(a). A 1x2 MMI was used to split the incoming signal into two arms, one of which is delayed with respect to the other. These are then fed into the two input ports of the 90° hybrid, producing an interferogram at each of the outputs as the input wavelength is scanned. We used a fiber array to simultaneously acquire the interferograms at the four outputs in a single sweep. Using a minimum phase technique¹⁷ we extracted both the CMRR and the hybrid phase error, as defined by equations (1) and (2), from this interferogram. The measurement results are shown in Fig. 6(b) and (c). The device exhibits a phase error below 5° in a 55nm bandwidth, and a CMRR clearly below -20dBc in 45nm bandwidth. Notice that the lower limit of the bandwidth is given by the tuning range of our laser.

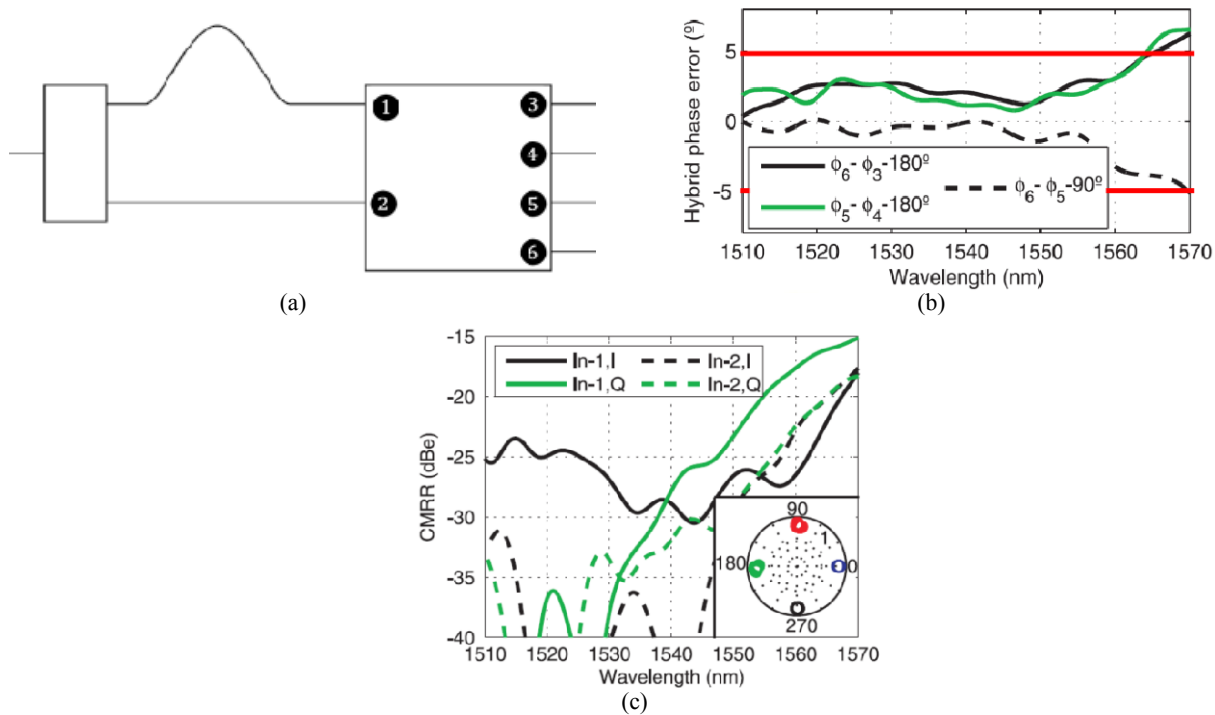


Figure 6. (a) On-chip interferometric test structure used to measure the amplitude and phase response of the 90° hybrid. (b) Measured hybrid phase error. (c) Measured CMRR.

7. CONCLUSIONS

We have discussed the need for coherent optical receivers, as well as the general structure of an optical receiver frontend. The optical 90° hybrid is a crucial element of such frontends and is preferably implemented with MMIs. The design of such couplers in Si-wire technology, is, however, challenging, owing to the strong lateral index contrast, that hampers image formation. We have shown that by reducing the etch depth in the multimode region the performance of Si-wire MMIs can be drastically improved. Furthermore, using fully etched input and output waveguides results in an ultra-compact device. The device was fabricated and measured with an on-chip interferometer, yielding a phase error below 5° and a CMRR better than -20dBe in a $\sim 50\text{nm}$ bandwidth.

ACKNOWLEDGEMENTS

This work was supported by the Spanish Ministerio de Ciencia (project TEC2009-10152), the Andalusian Regional Ministry of Science, Innovation and Business (project P07-TIC-02946), and the European Mirthe project (FP7-2010-257980).

REFERENCES

- [1] Ip, E., Lau, A., Barros, D., and Kahn, J., "Coherent detection in optical fiber systems", *Opt. Express* 16, 753-791 (2008)
- [2] Seimetz, M. and Weinert, C., "Options, feasibility, and availability of 2×4 90° hybrids for coherent optical systems", *J. Lightwave Technol.* 24, 1317-1322 (2006)
- [3] "Implementation Agreement for Integrated Dual Polarization Intradyne Coherent Receivers," Optical Internetworking Forum, 2010. Available: http://www.oiforum.com/public/documents/OIF_DPC_RX-01.0.pdf

- [4] Jeong, S., and Morito K., "Compact optical 90° hybrid employing a tapered 2×4 MMI coupler serially connected by a 2×2 MMI coupler", *Opt. Express* 18, 4275-4288 (2010)
- [5] Doerr, C.; Gill, D.; Gnauck, A.; Buhl, L.; Winzer, P.; Cappuzzo, M.; Wong-Foy, A.; Chen, E. & Gomez, L. "Monolithic Demodulator for 40-Gb/s DQPSK Using a Star Coupler", *J. Lightwave Technol.* 24, 171-174 (2006)
- [6] Soldano, L., and Pennings, E., "Optical Multi-Mode Interference Devices Based on Self-Imaging: Principales and Applications", *J. Lightwave Technol.* 13, 615-627 (1995)
- [7] Tang, Y.; Dai, D. & He, S., "Proposal for a Grating Waveguide Serving as Both a Polarization Splitter and an Efficient Coupler for Silicon-on-Insulator Nanophotonic Circuits", *IEEE Photonics Technol. Lett.* 21, 242-244 (2009)
- [8] Halir, R.; Vermeulen, D. & Roelkens, G., "Reducing Polarization-Dependent Loss of Silicon-on-Insulator Fiber to Chip Grating Couplers", *IEEE Photonics Technol. Lett.* 22, 389 -391 (2010)
- [9] Vivien, L., Osmond, J., Fédéli, J.-M., Marris-Morini, D., Crozat, P., Damlencourt, J.-F., Cassan, E., Lecunff, Y., Laval, S., "42 GHz p.i.n Germanium photodetector integrated in a silicon-on-insulator waveguide", *Opt. Express* 17, 6252-6257 (2009)
- [10] Halir, R.; Molina-Fernández, I.; Ortega-Moñux, A.; Wangüemert-Pérez, J. G.; Xu, D.-X.; Cheben, P. and Janz, S., "A Design Procedure for High Performance, Rib Waveguide based Multimode Interference Couplers in Silicon-on-Insulator", *J. Lightwave Technol.* 26, 2928-2936 (2008)
- [11] Huang, Z.; Scarmozzino, R. & Osgood, R. "A new design approach to large input/output number multimode interference couplers and its application to low-crosstalk WDM routers", *IEEE Photonics Technol. Lett.* 10, 1292-1294 (1998)
- [12] Thomson, D.J., Hu, Y., Reed, G. T., and Fedeli, J.-M., "Low Loss MMI Couplers for High Performance MZI Modulators," *IEEE Photonics Technol. Lett.* 22, 1485 -1487 (2010)
- [13] Hosseini, A., Subbaraman, H., Kwong, D., Zhang Y., and Chen, R.T., "Optimum access waveguide width for 1xN multimode interference couplers on silicon nanomembrane", *Opt. Lett.* 35, 2864-2866 (2010)
- [14] Halir, R., Roelkens, G., Ortega-Moñux, A., Wangüemert-Pérez, J.G., "High performance 90 hybrid based on a silicon-on-insulator multimode interference coupler," *Opt. Lett.* 36, 178-180 (2011)
- [15] Available at: <http://www.epixfab.eu>.
- [16] Roelkens, G., Vermeulen, D., Selvaraja, S., Halir, R., Bogaerts, W., and Thourhout, D., "Grating-Based Optical Fiber Interfaces for Silicon-on-Insulator Photonic Integrated Circuits," *IEEE J. Sel. Top. Quantum Electron.* 17, pp. 571-580 (2011)
- [17] Halir, R., Ortega-Moñux, A., Molina-Fernández, Í., Wangüemert-Pérez, J. G., Cheben, P., Xu D.-X., Lamontagne, B., and Janz, S., "Integrated Optical Six-Port Reflectometer in Silicon-on-Insulator", *IEEE J. Lightwave Technol.* 27, pages 5405-5409 (2009)